Hindawi
International Journal of Aerospace Engineering
Volume 2019, Article ID 9267059, 17 pages
https://doi.org/10.1155/2019/9267059

Research Article

H_∞ Control-Based Robust CAS Design for QTW-UAV via the Multiple-Model Approach with Particle Swarm Optimization

Chiramathe Nami,[1] Koichi Oka,[1] Masayuki Sato,[2] Akinori Harada,[1] and Koji Muraoka[2]

[1]*Department of Intelligent Mechanics and Aerospace Control, Kochi University of Technology, Kochi 782-0003, Japan*
[2]*Japan Aerospace Exploration Agency, Mitaka, Tokyo 181-0015, Japan*

Correspondence should be addressed to Koichi Oka; oka.koichi@kochi-tech.ac.jp

Received 13 September 2018; Revised 10 December 2018; Accepted 23 December 2018; Published 21 July 2019

Academic Editor: Paul Williams

Quad-Tilt-Wing (QTW) Unmanned Aerial Vehicle (UAV) is one of the promising types of UAVs because of its high-speed cruise performance similar to fixed-wing aircraft and VTOL (Vertical TakeOff and Landing) ability like helicopters. The control performance of our previously designed Control Augmentation System (CAS) for the aircraft was not satisfactory due to the oscillatory motions in flight tests. This paper thus presents an H_∞ control-based robust CAS design for QTW-UAV via multiple-model approach with Particle Swarm Optimization (PSO) to suppress the oscillatory motions. Although the adoption of the multiple-model approach to obtain robust CAS gains is the same as in our previous design, our new method has two unique features in contrast to the previously used method, that is, the design requirement for CAS gains is given in the frequency domain to shape the frequency responses from attitude command to attitude error and PSO is used to reduce the numerical complexity coming from a brute-force method, i.e., the gridding method. The overall control performance of the designed CAS gains is examined by human-in-the-loop nonlinear flight simulations. As an extension of the proposed method, we consider the situation in which uncertainty models with different probabilistic densities should be incorporated into the nominal model and show that the nominal performance can be improved at the expense of slight performance degradation for the models with small probabilistic density.

1. Introduction

Unmanned Aerial Vehicle (UAV) has gained much attention among researchers for the last two decades [1–3]. Quad-Tilt-Wing Unmanned Aerial Vehicle (QTW-UAV) has been considered as one of the promising tools for numerous fields of applications, because of its wide ability like hovering similar to helicopters and high-speed cruise similar to fixed-wing aircraft. Japan Aerospace Exploration Agency (JAXA) has thus designed and developed a series of QTW-UAVs (McART2 [4], AKITSU [5], and McART3 [6]) for their practical service. AKITSU, which is a practically sized QTW-UAV, successfully flied from a helicopter mode to an airplane mode and vice versa; however, oscillatory motions were found in both longitudinal and lateral-directional motions in some particular flight conditions [5].

Similarly to AKITSU, oscillatory motions were found during the flight test of McART3 [6]. To clarify this drawback, a flight result is shown in Figure 1. This indicates that some oscillatory motions were found in roll control and pitch control. In particular, roll oscillations appear in the latter half of the time history. Hence, it should be suppressed for safe flight. This paper is aimed at solving this problem.

The CAS gains in [5, 6] are designed to be robust against the supposed modeling errors via multiple-model approach [7], that is, using multiple models composed of a nominal model and slightly perturbed (off-nominal) models, CAS gains which are common to all of the models are designed. (More details on the multiple-model approach will be given in the next section.) However, the drawbacks of the CAS design in those papers are twofold, i.e., time domain design and optimization method. They are summarized

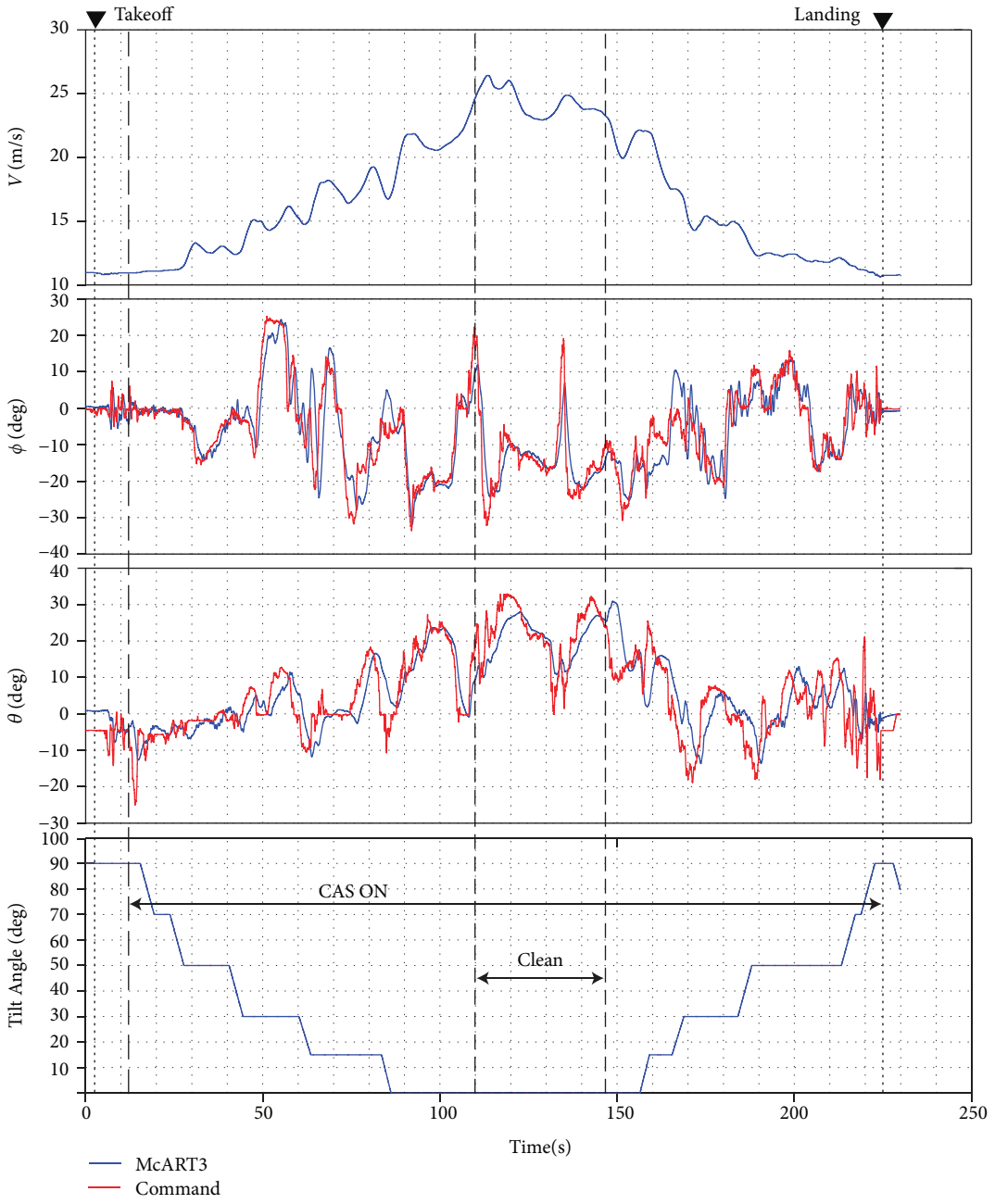

Figure 1: Time history of McART3 full conventional flight with a flight controller in [6].

below. Controller gains are designed in the time domain to realize satisfactory tracking performance. This is done by minimizing the worst or the average performance of the error between attitude (roll and pitch angles) and its step-type input command among all possible models. In this framework, it is difficult to prevent the oscillatory motions as shown in the flight tests for both QTW-UAVs. This is because it is not so straightforward to impose constraints in the time domain for suppressing oscillatory motions. The other drawback is the numerical complexity for designing CAS gains, that is, CAS gains are optimized by brute-force method, i.e., grid search method. Currently used CAS has only two gains (proportional and integral gains) in the longitudinal as well as lateral-directional motions, and thus, the numerical burden for its design is not so severe; however, when the controller ranges are wide and/or the number of the controller gains increases, large numerical complexity will be undoubtedly required. Furthermore, when the complicated CAS is adopted to enhance control performance, this might be unavoidably problematic.

To overcome these drawbacks, this paper proposes a design method with frequency domain constraints with reduced numerical complexity for the optimization, that is, robust CAS gains are designed by shaping the sensitivity function within the H_∞ control framework using multiple models as in [6] and Particle Swarm Optimization (PSO)

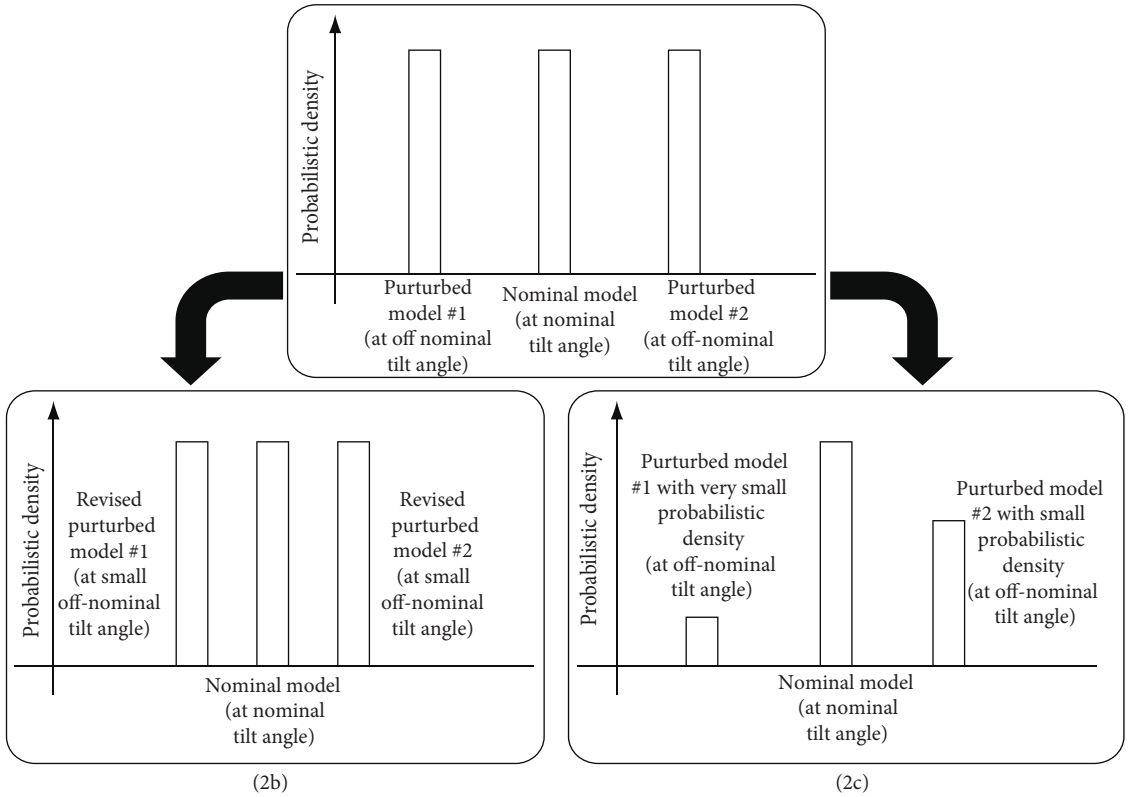

Figure 2: Conceptual figure of our method with a priori-given probabilistic density.

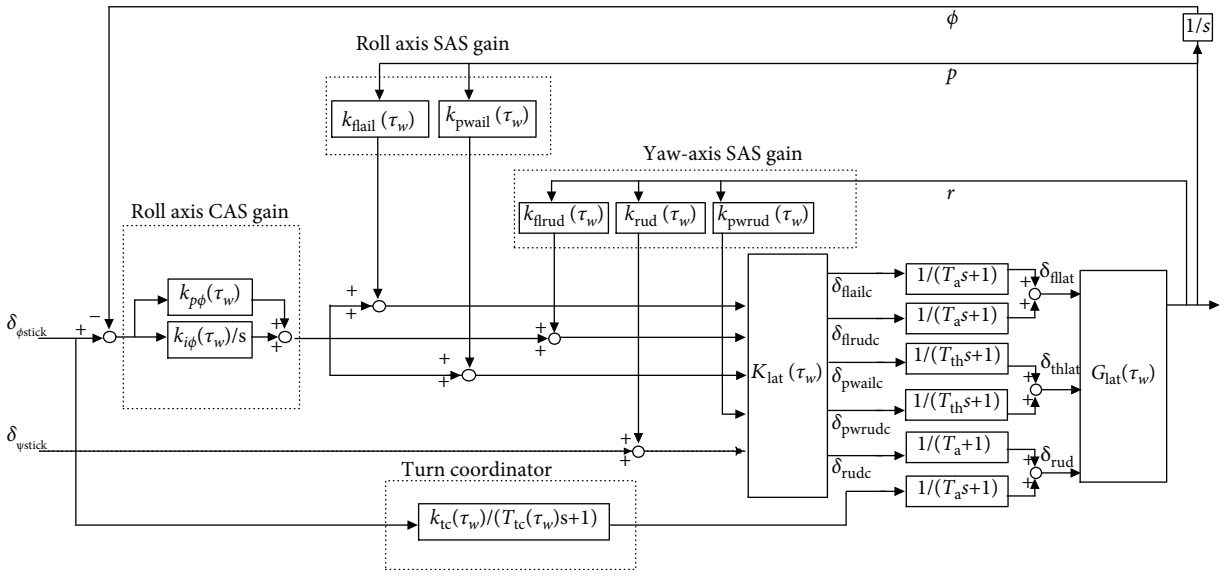

Figure 3: Block diagram for lateral-directional motion control of McART3 used in [6].

algorithm [8–10]. The PSO algorithm, which is one of the oriented search algorithms, is used as an alternative to the brute-force method with small numerical complexity. As shown in [11], PSO is more effective than Genetic Algorithm (GA), which is one of the most famous metaheuristic methods, in terms of computation time. Furthermore, PSO can be easily applied to the problems in which cost functions are nonsmooth with respect to controller gains to be designed, because it needs neither gradient nor derivative of cost functions. For those reasons, we adopt the PSO algorithm in this paper.

Robust CAS gains which suppress oscillatory motions are obtained by our new method, and the performance is consequently verified through human-in-the-loop nonlinear simulations with/without wind gust.

We only show the results for the lateral-directional motions in this paper. This is because, although the same problem for the longitudinal motions was addressed,

Table 1: McART3 nominal models and perturbed models ("N" denotes "nominal" and "P" denotes "perturbed" models) and SAS gains in lateral directional motions ("-" denotes disuse).

Design point (tilt angle)	Model name	Tilt angle	SAS gain $k_{\text{flail}}(\tau_w)$	$k_{\text{pwail}}(\tau_w)$	$k_{\text{frud}}(\tau_w)$	$k_{\text{rud}}(\tau_w)$	$k_{\text{pwrud}}(\tau_w)$
1 (T90)	1 - N	90	—	29	86	—	—
	1 – $P1$	80					
2 (T70)	2 - $P1$	80	0	29	86	100	—
	2 – N	70					
	2 – $P2$	60					
3 (T50)	3 - $P1$	60	103	40	86	100	—
	3 – N	50					
	3 – $P2$	40					
4 (T30)	4 – $P1$	40	83	40	86	100	—
	4 – N	30					
	4 – $P2$	20					
5 (T15)	5 - $P1$	20	67	33	86	100	—
	5 – N	15					
	5 – $P2$	10					
6 (T00)	6 - $P1$	10	46	—	—	150	89
	6 – N	0 (flap down)					
	6 – $P2$	0 (clean)					
7 (clean)	7 - $P1$	0 (flap down)	46	—	—	150	45
	7 – N	0 (clean)					

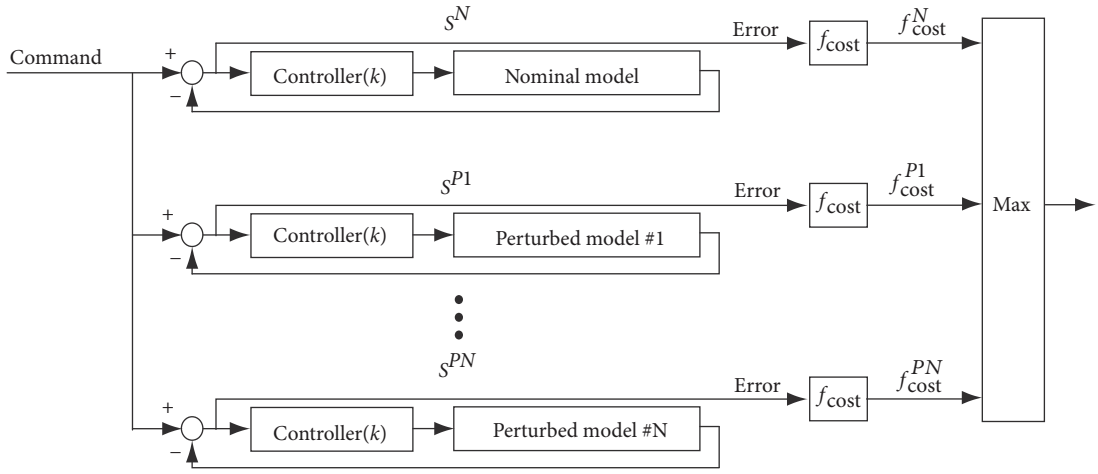

Figure 4: Concept of the multiple-model approach for designing robust controller gain k.

oscillatory motions were hardly suppressed due to the severe constraints for admissible gain intervals which come from hardware constraints for possible and expected motions; however, we would like to emphasize that our approach can be applied to the controller design for the longitudinal motions as well as other-type aircraft motion control. The reason is that the inapplicability for the longitudinal motions comes from only the strictly regulated admissible gain intervals and they can be easily relaxed if up-to-date sensors with high precision are implemented. In contrast to our preliminary results in [12], this paper focuses on the robustification of our proposed method in [12] by incorporating the multiple-model approach and on the verification of our achievement via human-in-the-loop nonlinear flight simulations. The CAS gains in [12] are designed only for the nominal models and consequently have no robustness against the possible modeling errors. Thus, the design of robust CAS gains

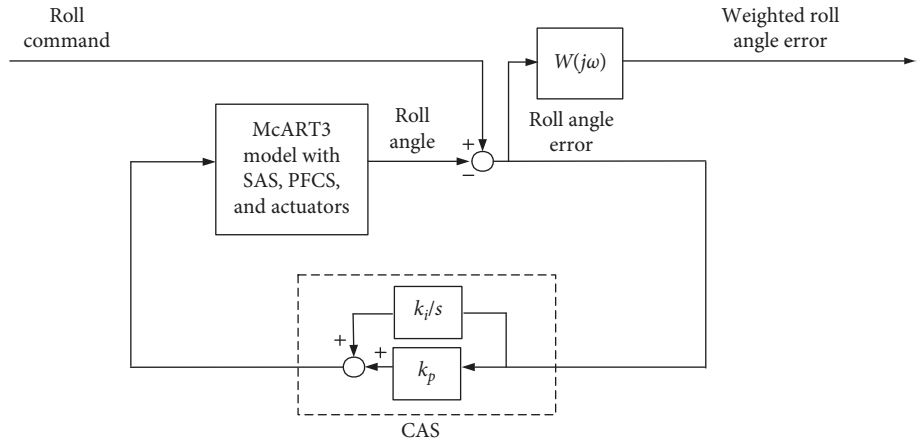

Figure 5: Block diagram for our CAS design.

and its verification by human-in-the-loop nonlinear simulations are the main contributions of this paper.

In addition, we also show an extension of our method. Let us consider the situation in which satisfactory controller gains cannot be obtained via multiple-model approach. If the perturbations of off-nominal models are set as larger than the required design specifications for sufficient safety, then, one remedy is to set the perturbations of the perturbed models from the nominal condition smaller, as in Figure 2(b), that is, smaller perturbations are supposed; however, this remedy might lead to very fragile controllers. Another remedy is to set the possibility of the occurrence of the perturbed models smaller than that of the nominal model as in Figure 2(c), if the possibility of the perturbed models is supposed to be smaller than that of the nominal model. In this case, the probabilistic density for the perturbed models must be given a priori; however, if it is given, nonfragile controller gains can be obtained and it is possible to improve the nominal performance at the expense of slightly deteriorated performance for the perturbed models. The effectiveness of this extension is confirmed by a design example with linear simulations.

2. Controller Design

In this section, the basic flight controller of McART3 and its design are first summarized. Second, our proposed method to enhance the oscillatory suppression ability for the controller is described. Finally, the description of our optimization algorithm, i.e., the PSO algorithm, is given.

2.1. Previous Design of the Flight Controller. In [6], the flight controller for the lateral-directional motions of McART3 is designed to satisfy the following three requirements:

(i) Safe flight controlled by a remote ground pilot

(ii) Adaptation to variation in aerodynamic characteristics caused by wing tilt angle changes

(iii) Guarantee of robust performance against possible modeling errors

Table 2: Admissible CAS gain regions, CAS gains in [6], optimized CAS gains using our method and the parameters of weighting function $W(j\omega)$.

Design point	K_{lat}		Gains in [6]		Our CAS gains		ω_c	HF
	k_p	k_i	$k_{p\phi}$	$k_{i\phi}$	$k_{p\phi}$	$k_{i\phi}$		
1 (T90)	[-50,0]	[-40,0]	-50	-40	-38	-34	0.2	1.44
2 (T70)	[-50,0]	[-40,0]	-50	-40	-40	-37	0.1	1.47
3 (T50)	[-80,0]	[-50,0]	-80	-50	-41	-19	0.2	1.67
4 (T30)	[-120,0]	[-50,0]	-88	-50	-41	-19	0.5	1.70
5 (T15)	[-100,0]	[-50,0]	-100	-50	-42	-26	0.4	1.21
6 (T00)	[-100,0]	[-50,0]	-100	-50	-55	-45	1.0	1.10
7 (clean)	[-100,0]	[-50,0]	-100	-50	-31	-22	0.6	1.05

To meet these requirements, we use the same solutions which are originally adopted in [5, 6] for (i), (ii), and (iii), that is, (1) the conventional Stability/Control Augmentation System (S/CAS) structure, (2) Gain-Scheduling (GS) technique, and (3) multiple-model approach, respectively, are adopted for the three requirements. For completeness, brief explanations of them are given below.

2.1.1. S/CAS Structure. Since McART3 has tilting wings, the aerodynamic characteristics vary significantly; however, the fundamental rules of its motion dynamics do not change from those of conventional aircraft. Thus, a well-established flight control structure, i.e., S/CAS including Turn Coordinator (TC), is adopted.

The block diagram of the used S/CAS is shown in Figure 3. The SAS gains, which are used to enhance the stability of McART3, are the same as the ones in [6]. For reference, the usage and the values of SAS gains are given in Table 1. The CAS consists of a command hold loop which has only two control gains, i.e., proportional gain and integral gain. Both of them are required to be designed. The TC is implemented for the reduction of lateral velocity in turns. To be more specific, TC is a first-

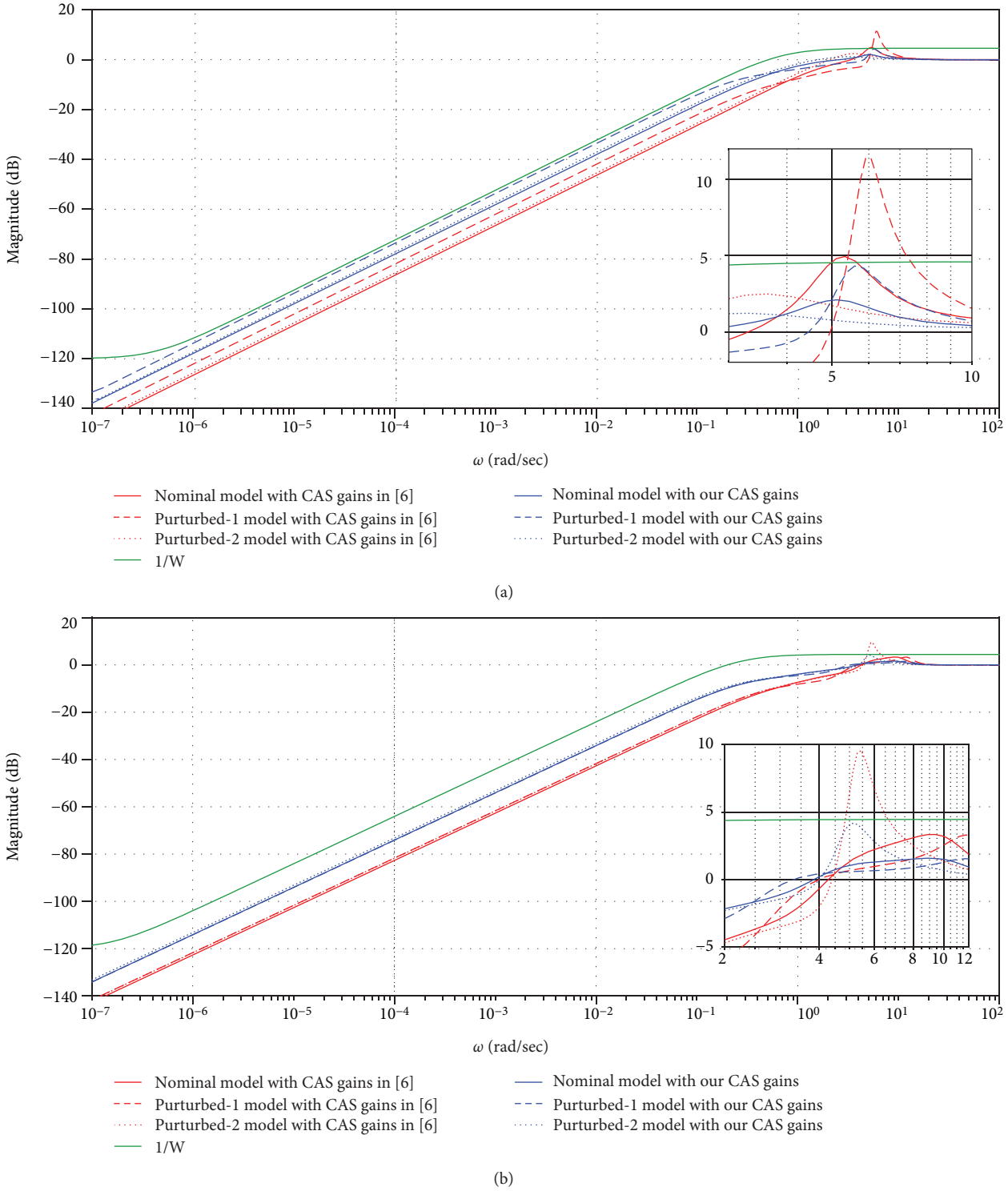

FIGURE 6: Gain plots of closed–loop sensitivity functions using CAS gains in [6], optimized gains in Table 2, and $1/|W(s)|$ at design point 4 (T30) (a) and design point 3 (T50) (b) (close–look figures at maximum peak gains are given in the boxes).

order filter which has the same structure as previously used in [6].

2.1.2. Gain-Scheduling (GS) Technique. In the flight controller design, gain-scheduling technique is commonly used to adapt to the changes of vehicle aerodynamic characteristics, e.g., large-scale helicopter [13] and aircraft with highly nonlinear behavior [14].

The conventional design technique for GS CAS is applied to McART3. The concrete procedure is given as follows: we first select seven design points (design points 1, 2, 3, 4, 5, and 6 at tilt angles of 90, 70, 50, 30, 15, and 0

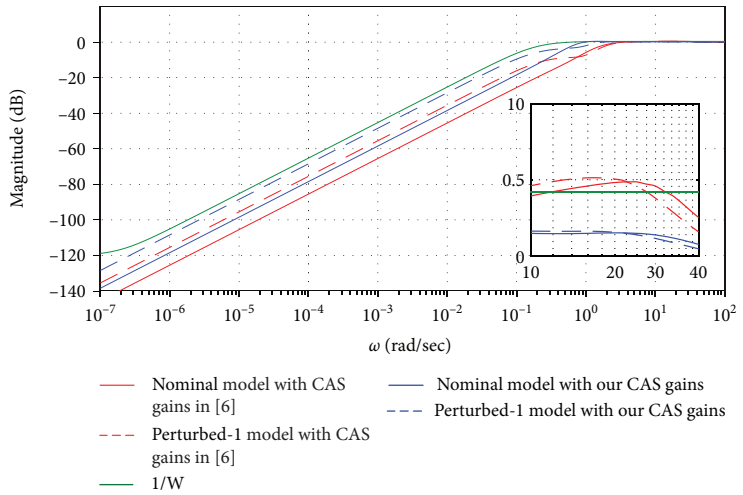

(a)

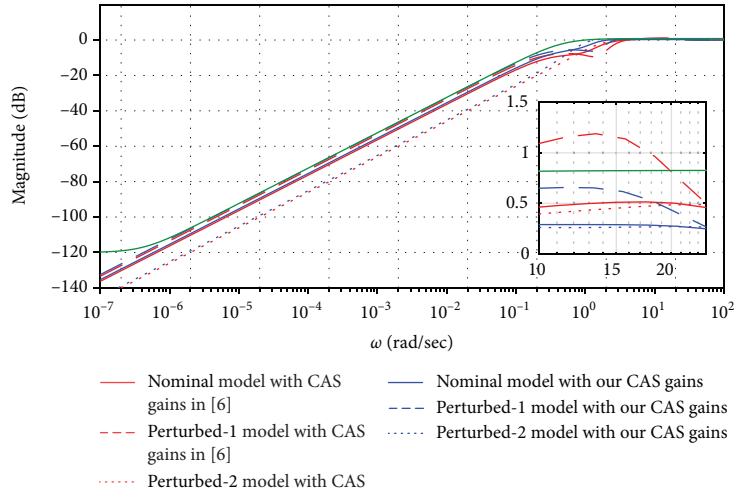

(b)

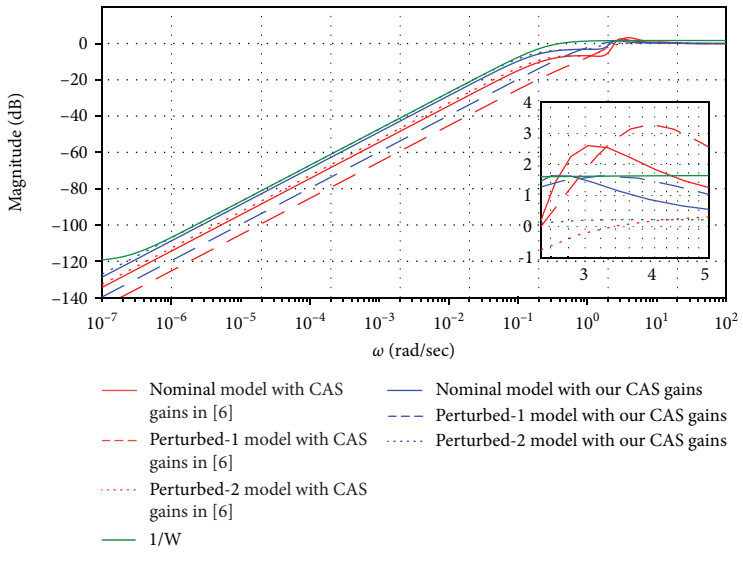

(c)

Figure 7: Continued.

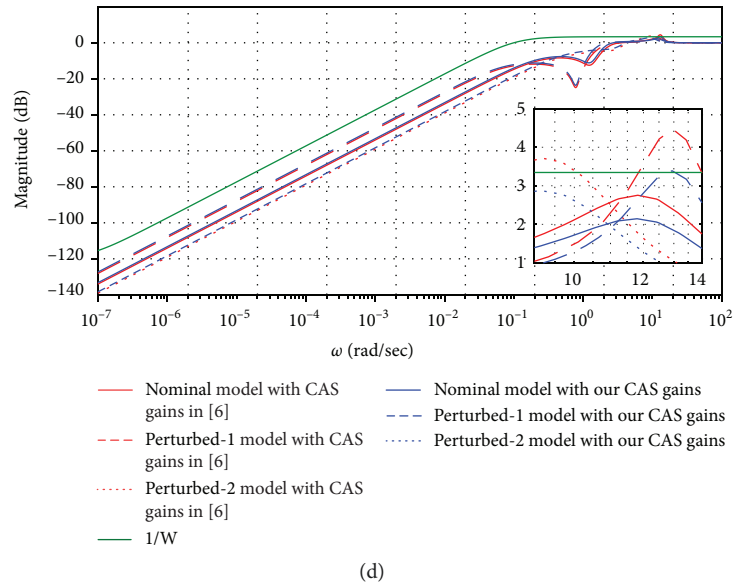

(d)

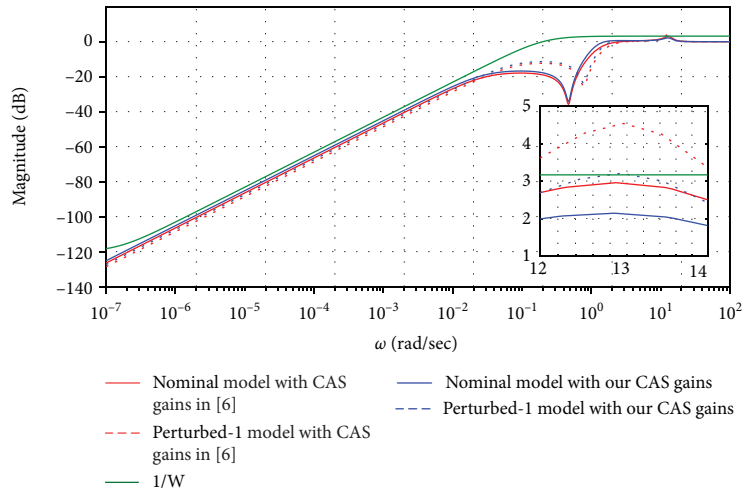

(e)

Figure 7: Gain plots of closed-loop sensitivity functions using CAS gains in [6], optimized gains in Table 2, and $1/|W(s)|$ in each design points. (a) Clean, (b) T00, (c) T15, (d) T70, and (e) T90. (close-look figures at maximum peak gains are given in the boxes.)

degrees, respectively, and design point 7 with clean configuration) as indicated in Table 1; then design controller gains at those design points; and finally obtain GS CAS by interpolating the obtained gains in a piecewise linear fashion.

2.1.3. Multiple-Model Approach. To design robust CAS gains, the multiple-model approach [7] is used, i.e., nominal model and perturbed models to represent the possible modeling errors are introduced, and common gains for all the models are designed to guarantee robust performance shown in Figure 4.

The idea of the multiple-model approach is simple and rational for designing practical controller gains. The concrete procedure is given below. We first set the nominal model as a nominal McART3 dynamics model with SAS; second, systems which are similarly generated at neighboring tilt angles are set as "perturbed models" (indicated in Table 1) to represent the possible modeling errors; finally, common CAS gains for those models are designed to guarantee robust performance by solving the following problem with an appropriately defined cost function $f_{\text{cost}}(k)$ together with an appropriately defined admissible gain set K;

$$\min_{k \in K} \max_{\substack{\text{nominal and} \\ \text{perturbed models}}} f_{\text{cost}}(k). \tag{1}$$

This formulation attempts to design the optimal robust CAS controller gain with the worst cost among all supposed models being minimized. Therefore, it is expected that the designed gains have robustly optimized control performance against the supposed modeling errors which are represented by the multiple models.

By following almost the same design procedure as above, the flight controller of McART3 was successfully designed in

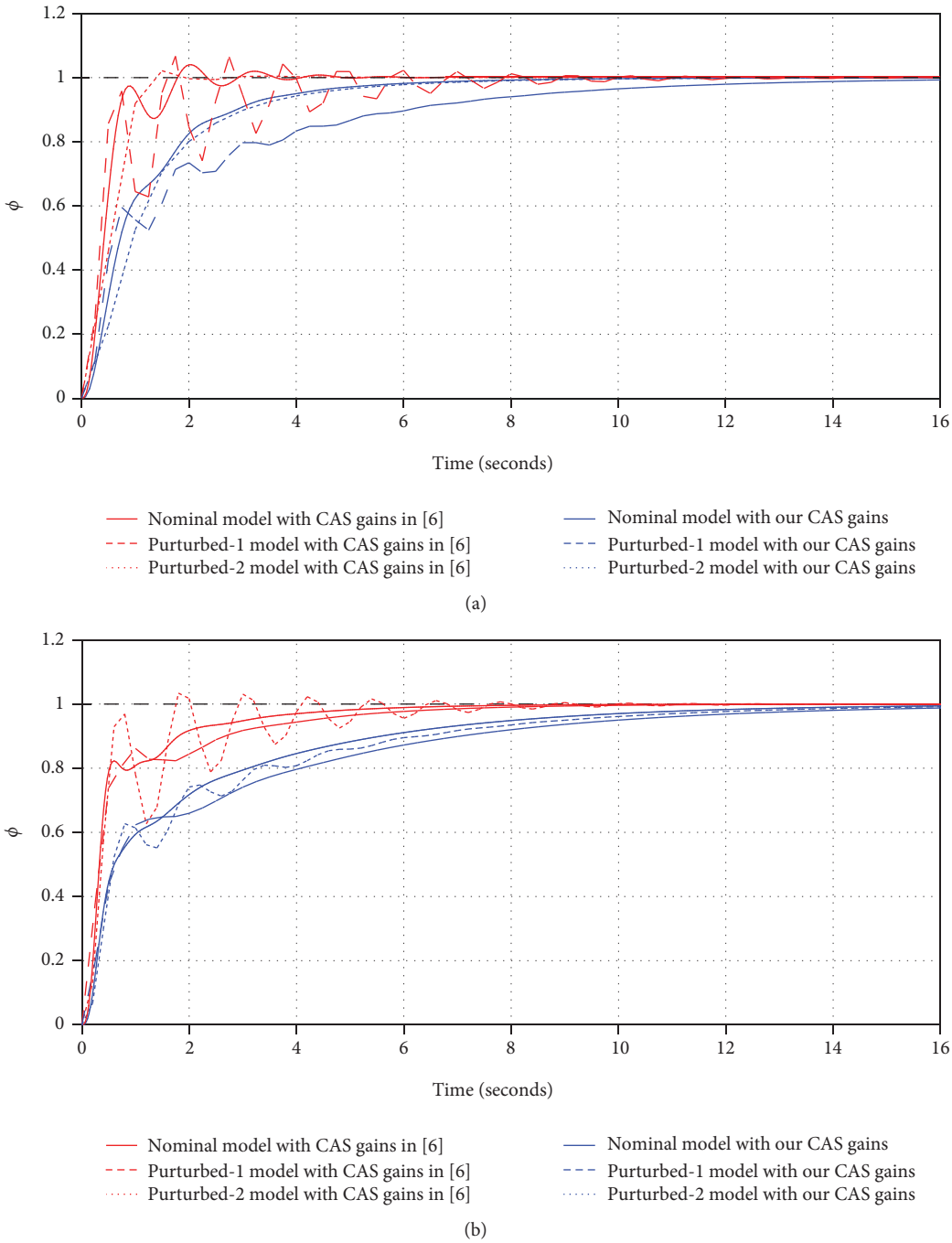

FIGURE 8: Step responses using oscillation suppressing CAS gains in Table 2 and CAS gains in [6] at design point 4 (T30) (a) and design point 3 (T50) (b).

[6]; however, the oscillatory motions were sometimes large and they should be suppressed for flight safety. Hence, an additional requirement for oscillatory motion suppression is introduced and a method to meet the requirement is integrated into the method in [6].

2.2. Proposal of Shaping Sensitivity Function in the CAS Design to Suppress Oscillatory Motions. We use sensitivity function shaping [12, 15] within the H_∞ control framework to meet the additional requirement, that is, suppression of oscillatory motions. Hereafter, it is referred as another requirement:

(iv) Suppression of oscillatory motions by shaping sensitivity functions within the H_∞ control framework

We propose a method to design robust structured CAS gains to suppress the oscillatory motions by shaping sensitivity function with multiple models incorporated. By using the block diagram in Figure 5, we consider the sensitivity

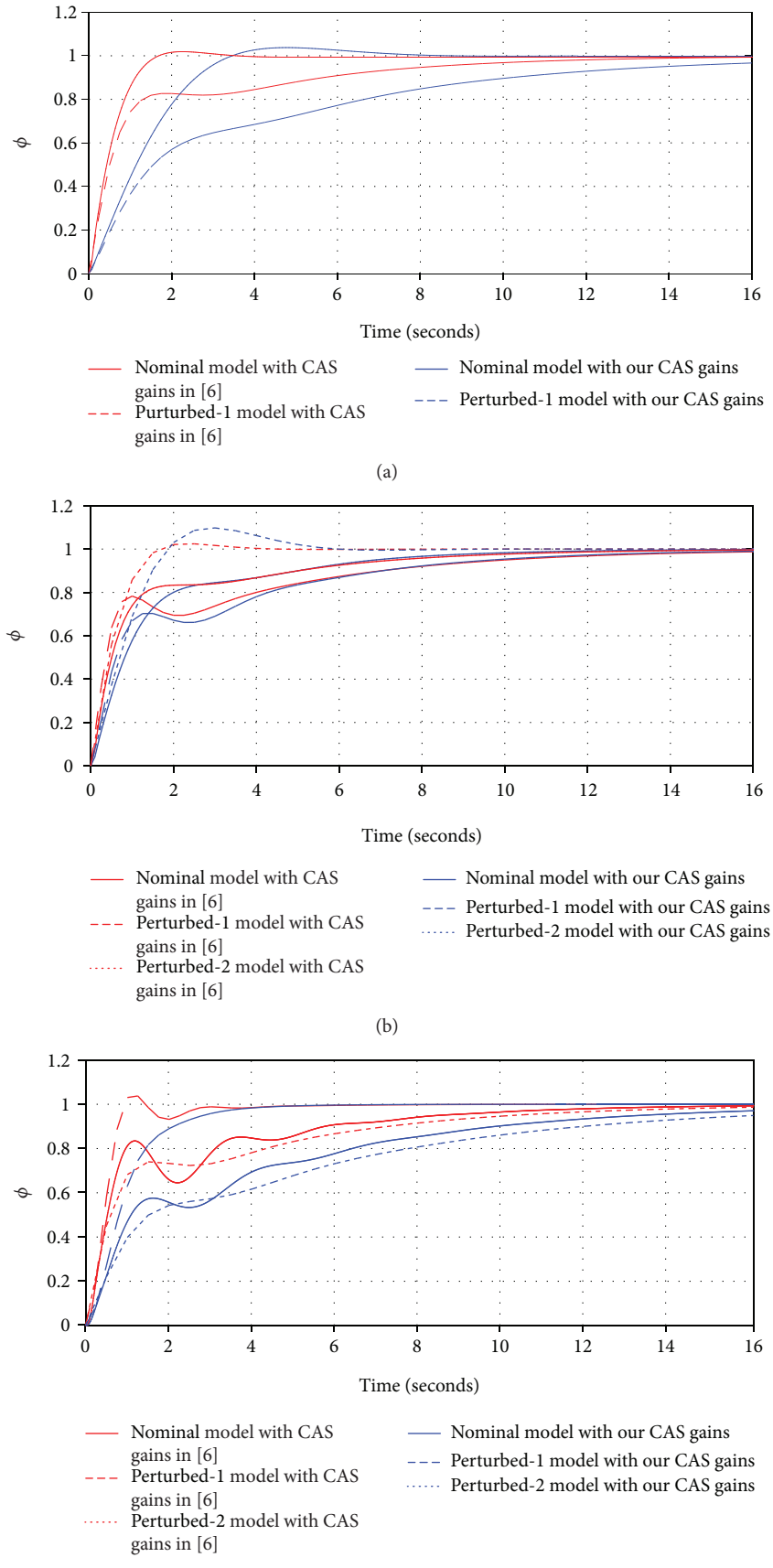

Figure 9: Continued.

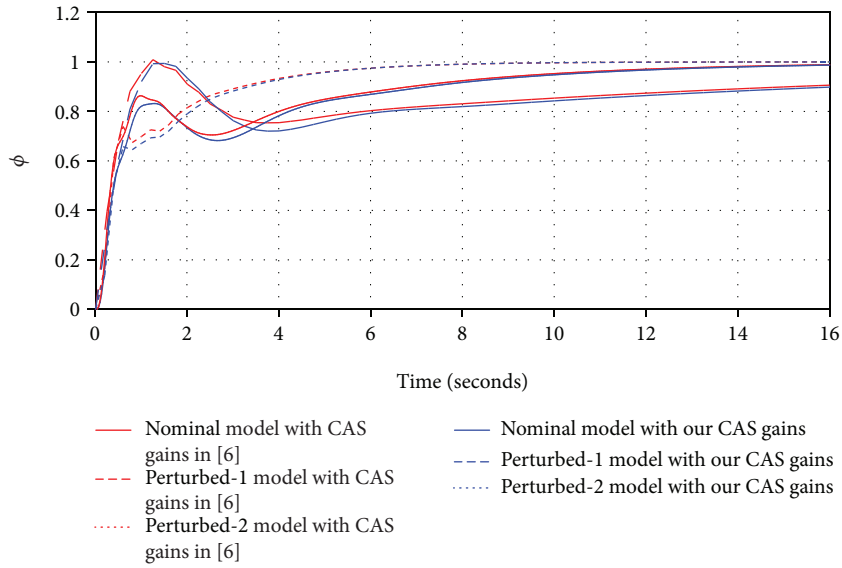

(d)

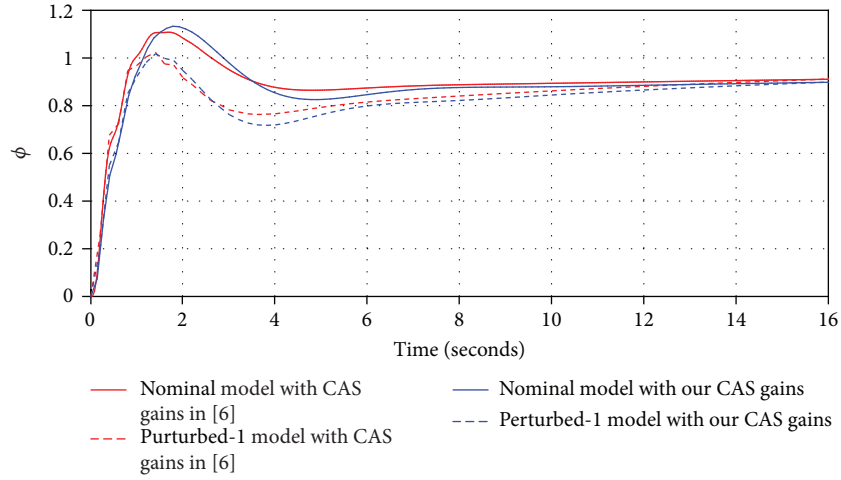

(e)

Figure 9: Step responses of using oscillation suppression CAS gains in Table 2 and CAS gains in [6] at (a) clean, (b) T00, (c) T15, (d) T70, and (e) T90.

function $S(j\omega)$ defined as a transfer function from roll command to roll angle error. To shape this sensitivity function, an appropriately defined weighting function $W(j\omega)$ for oscillation suppression is introduced.

Then, the cost function in Figure 4, i.e., f_{cost}, is defined as the H_∞ norm of the weighted sensitivity function, that is,

$$f_{\text{cost}}(k) = \|W(j\omega)S(j\omega)\|_\infty. \tag{2}$$

Thus, we define our optimization problem as follows;

$$\min_{k\in K} \max_{\substack{\text{nominal and} \\ \text{perturbed models}}} \|W(j\omega)S(j\omega)\|_\infty. \tag{3}$$

Solving the above optimization problem with an appropriate weighting function $W(j\omega)$ produces nonoscillatory robust CAS gain vector k which minimizes the worst weighted sensitivity function among all supposed plant models.

Table 3: k_{tc} gains in [6], T_{tc} using our CAS gains in Table 2, and evaluation time T_{eval} in equation (5) (TC is not used at T70 and T90).

Design point	k_{tc} gains in [6]	Optimized T_{tc}	T_{eval} (sec)
3 (T50)	2.8118	0.8216	5
4 (T30)	1.4198	1.1326	5
5 (T15)	1.0567	1.7257	5
6 (T00)	0.5230	0.2502	10
7 (clean)	0.2904	0.2031	5

2.3. Particle Swarm Optimization. Eberhart and Kennedy [8] proposed an optimization concept for continuous nonlinear functions using particle swarm methodology which was inspired by the simplified movement behavior of organisms in a bird flock or fish school. With regard to this algorithm, a term "particles" is used to represent candidates of the solutions to the problem. A unique property

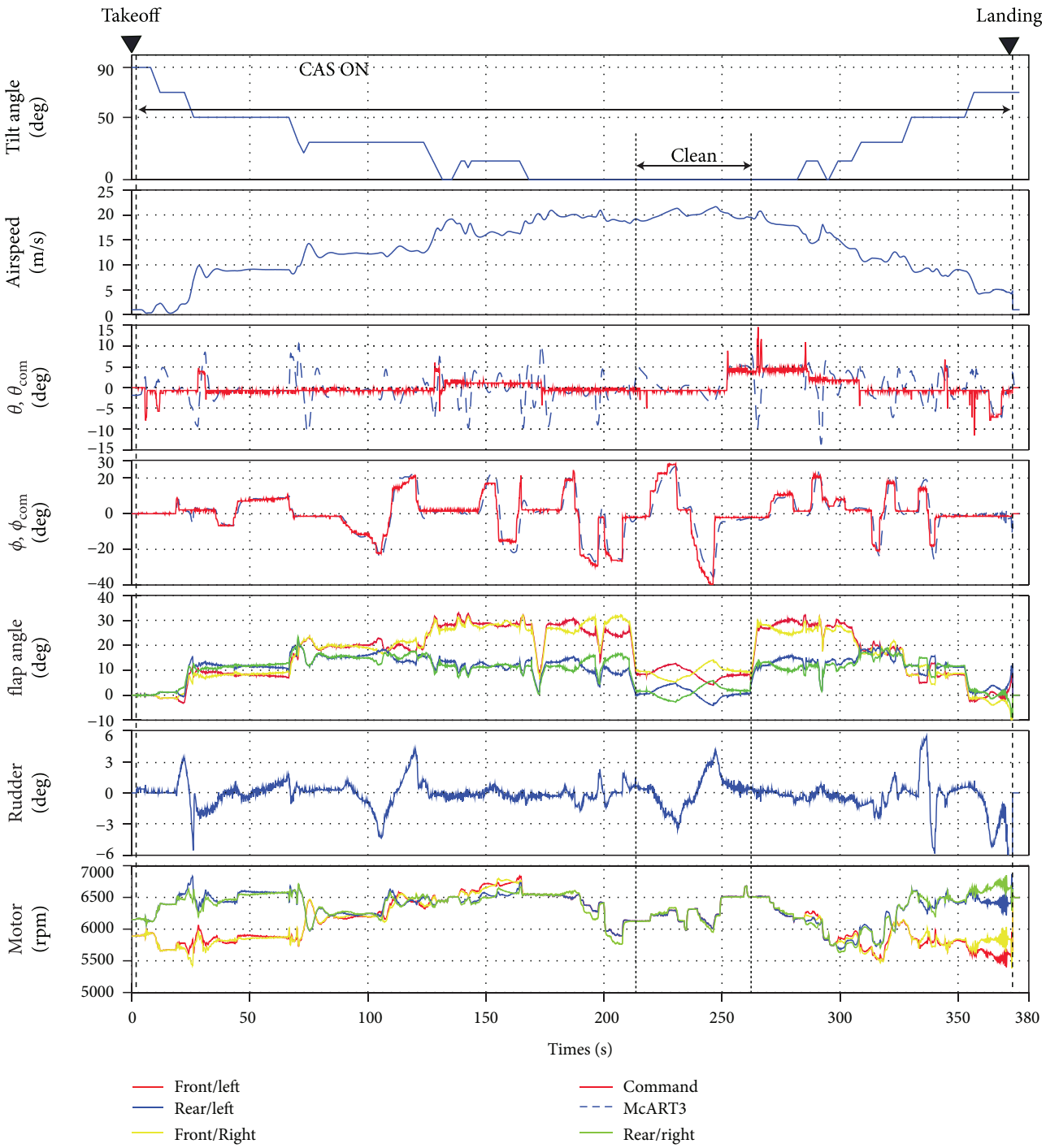

Figure 10: Time history of human-in-the-loop flight simulation without wind gust.

of this algorithm is that not only the local optima obtained by each particle at all previous iteration steps but also the global optimum obtained by whole particles, i.e., swarm, at the current iteration step are both used to update the candidates.

The PSO algorithm needs no smoothness of the cost function with respect to design variables; hence, various constraints (including linear and/or nonlinear intervals for the design variables) can be easily incorporated into the problem by suitable definition of cost functions [16]. Therefore, various design problems, e.g., nonconvex optimization problems [17], optimization problems with equality/inequality constraints [18], and structured controller design problems [16, 19, 20] have been solved using the PSO algorithm.

3. Design Results

We show the design results for the oscillation-suppressing robust CAS and consequently show a posteriori check via human-in-the-loop nonlinear simulations. Then, we show

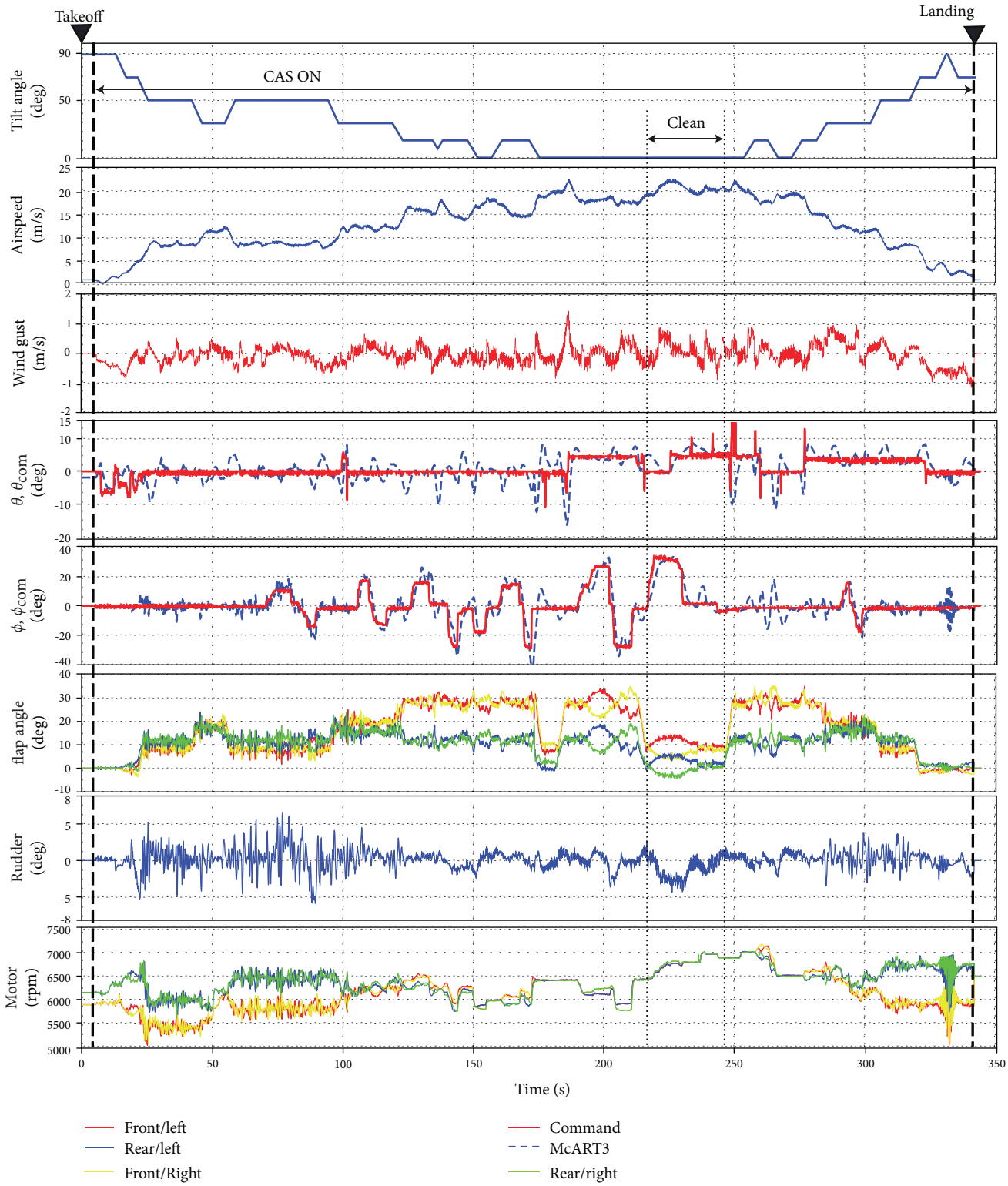

Figure 11: Time history of human–in–the–loop flight simulation under gusty condition using Dryden model.

an extension of our proposed method, i.e., nominal performance improvement in exchange for slight performance degradation for perturbed models with small probabilistic density.

After several trial and errors, we finally set the number of swarms and the maximum iterations in our design as 20 and 20 iterations, respectively. They are slightly small compared to the numbers in literature (e.g., [16]); however, we only design two parameters (proportional and integral gains) and found that our setting was enough to obtain the exposed results.

Table 4: Scaling factors for weighting functions.

	c_N	c_{P1}
Case 1	1	1
Case 2	1	0.7

3.1. Oscillation-Suppressing Robust CAS. We show our chosen weighting function $W(j\omega)$ and consequently show design results. Next, a corresponding TC design result is shown. Finally, human-in-the-loop nonlinear simulations are demonstrated.

3.1.1. Weighting Function. Weighting function $W(j\omega)$ is crucial to meet our additional requirement (iv), i.e., oscillation suppression, because $W(j\omega)$ shapes the sensitivity function $S(j\omega)$; however, it is not realistic to set an appropriate weighting function just by one shot. Usually, it requires several trial and errors to set appropriate weighting functions in the H_∞ control. Thus, if the weighting function has a complicated form (e.g., high-order weighting functions), then, it may take a lot of time to determine the appropriate coefficients. We therefore select a first-order filter as the inverse of the weighting function which is characterized with only three parameters, Direct Current (DC) gain, cutoff frequency (ω_{coff}), and High-Frequency (HF) gain. In our design, DC gains of $W^{-1}(j\omega)$ are fixed as 1.0×10^{-6} to realize good tracking performance in low frequencies as in [6], while ω_{coff} and HF gains are left as the design parameters to be tuned. Consequently, the weighting functions have the form as follows:

$$W^{-1}(s) = \frac{\text{HF}s + 10^{-6}\omega_{\text{coff}}}{s + \omega_{\text{coff}}}. \tag{4}$$

The HF gain and ω_{coff} are particularly determined as follows: we first set the HF gain by trial and errors to reduce the peak gains which produce the problematic oscillatory motions; then, ω_{coff} is adjusted to enhance the tracking performance. These results are shown in Table 2, in which gain crossover frequency (ω_c) is shown instead of cutoff frequency (ω_{coff}) because gain crossover frequency straightforwardly represents the bandwidth of control performance.

In our design, different weighting functions are chosen at each design point for better control performance at each tilt angle.

Remark. Regarding the HF gain, if it is set as just above unity, it indeed reduces the peak gains; however, the designed CAS gains tend to have the property that step responses are too overdamped, that is, slow response and enlarged settling time. Hence, the HF gain must be appropriately chosen to suppress the oscillatory motions while good tracking performance is maintained.

3.1.2. Design Results and A Posteriori Analysis at Each Design Point. The weighting functions are finally set as in Table 2.

Table 5: The parameters of chosen $W(j\omega)$ for both case 1 and case 2 in Table 4, optimized CAS using our method, and H_∞ norms at design point 7 (* indicates the model which has worse performance).

	Design point 7 (clean) $\omega_c = 0.8$, HF = 1.1			
	$k_{p\phi}$	$k_{i\phi}$	$c_N \|W(j\omega)S_N(j\omega)\|_\infty$	$c_{P1}\|W(j\omega)S_{P1}(j\omega)\|_\infty$
Case 1	-43.6	-38.0	0.9446	0.9664*
Case 2	-44.0	-26.9	0.9338*	0.9203

We consequently obtain the control gains in Table 2. The gains tend to be less than the results in [6], and they are not so close to the boundaries of the admissible CAS gain intervals comparing to the results in [6].

We next conduct a posteriori analysis to confirm the reduction of the peak gains with our CAS gains. In Figure 6, the gain plots of the sensitivity function at design points 3 and 4 are shown. (Other gain plots of the sensitivity functions are given in Figure 7.) For reference, in the figure, gain plots of the sensitivity functions using CAS gains in [6] are also shown. The results confirm that the peak gains which cause the oscillatory motions are indeed reduced compared to the results in [6]. In particular, Figure 6(a) shows the reduction of the maximum peak gain (Perturbed-1 model) from 11.4 dB at 6.06 rad/sec to 4.32 dB at 5.59 rad/sec and Figure 6(b) shows the reduction of the maximum peak gain (Perturbed-2 model) from 9.56 dB at 5.45 rad/sec to 4.18 dB at 5.06 rad/sec.

We next check the achievement of our objective in the time domain, that is, we next check if the oscillatory motions are suppressed with our CAS gains for step command. In Figure 8, the step responses at design points 3 and 4 are shown. (Other step responses are given in Figure 9.)

In the figure, for reference, the step responses using CAS gains in [6] are also shown. This figure confirms that the oscillatory motions are suppressed compared to the results with CAS gains in [6] in exchange for a slower response. (Note that we could not improve tracking performance anymore.)

In summary, we have confirmed that requirements (iii) and (iv) are met by our method. The GS CAS is obtained by interpolating the gains in a piecewise linear fashion.

3.1.3. TC Design for Oscillation-Suppressing CAS. By following the TC calculation procedure in [5], we design the TC. The gains $k_{\text{tc}}(\tau_w)$ are identical as in [6] because the same SAS gains as in [6] are used. On the other hand, $T_{\text{tc}}(\tau_w)$ is obtained by optimizing the same cost function as in [5] which is given in equation (5) for the step input of $\delta_{\phi\text{stick}}$ using our CAS gains.

$$\int_0^{T\text{eval}} \nu^2 dt, \tag{5}$$

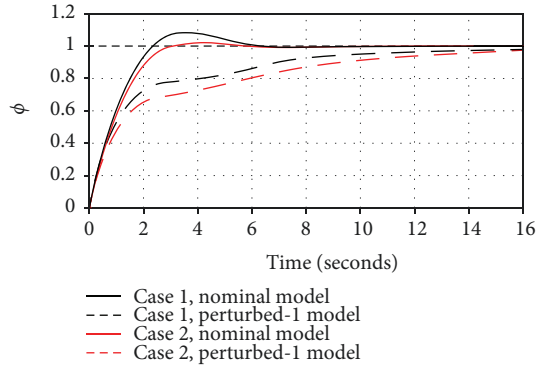

Figure 12: Step responses at design point 7 (clean) using CAS gains in Table 5.

where T_{eval} denotes the evaluation time defined a priori. We use the same values for T_{eval} as in [6]. The design results of T_{tc} are shown in Table 3 at each design point. Finally, the GS TC is obtained by interpolating the gains and time constants in a piecewise linear fashion.

3.1.4. Human-In-The-Loop Nonlinear Simulations. To examine the control performance in transition phases between different wing tilt angles, human-in-the-loop flight simulations, in which nonlinear equations and look-up aerodynamic coefficient tables are used, were conducted. These simulations were carried out by an amateur pilot who was familiar with QTW-UAVs. The pilot conducted accelerated transition from T90 to clean configuration and decelerated transition from clean configuration to T90 within a visual line of sight. This is because our main objective was to confirm that our CAS gains suppress oscillatory motions.

Figure 10 shows the simulation result without wind gust. In the figure, CAS was engaged from just after takeoff until landing which is denoted by a term "CAS ON".

The simulation results confirm that our designed CAS gains work well for all tilt angles, that is, McART3 flies safely in the helicopter mode, airplane mode, and transition mode. In particular, the roll angle faithfully follows its command in all tilt angles without oscillations; however, small delays are confirmed, in particular at, clean configuration, 15 and 30 degrees of tilt angles. It is consistent with our linear simulations. (Note that the oscillatory motion in pitch angles occurred at transition. This is because the same longitudinal CAS gains in [6] are used.) Furthermore, to confirm the practicality of our design CAS gains, human-in-the-loop flight simulations with wind gust were also conducted (see Figure 11). This simulation confirms that, under gusty condition which is one of the triggers for roll oscillations, our CAS gains also work well.

In summary, we have confirmed that our designed CAS gains work well in both gusty and calm conditions and the oscillatory motions in roll control are suppressed.

3.2. Extension to the CAS Design for Models with Different Probabilistic Densities. If the probabilistic density of the perturbed models and the nominal model is different as shown in Figure 2(c), then, we do not need to use the same weighting function for all models in the multiple-model approach. We now consider the situation in which the probabilistic density of the perturbed models is smaller than that of the nominal model. It is thus reasonable to use the same weighting function with different scaling factors multiplied.

The term "different scaling factors" for the weighting function can represent different probabilistic densities. For example, if the first perturbed model has just half the possibility of occurrence compared to the nominal model and the second perturbed model has only 25% possibility compared to the nominal model, then, it is reasonable to set the scaling factors for the nominal, first, and second perturbed models (i.e., c_N, c_{P1}, and c_{P2}) as 1, 0.5, and 0.25, respectively.

The cost function is thus modified accordingly, that is, $f_{\text{cost}}(k)$ in equation (3) is revised as follows:

$$f^i_{\text{cost}}(k) = c_i \| W(j\omega) S_i(j\omega) \|_\infty, \quad i = \{N, P1, P2\}, \tag{6}$$

where coefficient c_i must comply with the probabilistic density of the corresponding models.

This idea improves the performance of the nominal model in exchange for the performance degradations of the perturbed models which have smaller probabilistic density than the nominal one. We apply this methodology to design point 7 in Table 2 which has only two plant models, that is, nominal and its first perturbed model.

The scaling factors for the weighting function are set as shown in Table 4. We consequently obtain CAS gains as shown in Table 5. In the table, case 1, in which c_N and c_{P1} values are both set to unity, shows that the first perturbed model has worse performance than the nominal model; however, in case 2, in which the c_{P1} value is set to be smaller than the c_N value, the nominal model has worse performance.

We next examine the effectiveness of our CAS design in the time domain with step responses. In Figure 12, it is confirmed that, when the scaling factor of the weighting function for the first perturbed model is set to be smaller than the nominal model, the nominal performance increases in exchange of enlarged settling time for the first perturbed model.

4. Conclusions

To address the drawbacks in existing design methods for Quad-Tilt-Wing Unmanned Aerial Vehicle (QTW-UAV), i.e., oscillatory motions and large numerical complexity in controller gain design, this paper applies sensitivity function shaping approach within the H_∞ control framework to the Control Augmentation System (CAS) design. In this problem, the multiple-model approach is used to robustify the controller gains, using the Particle Swarm Optimization (PSO) algorithm. In contrast to the previous design method, design specification is given in the frequency domain to shape the frequency responses from attitude command to attitude error and nonoscillatory robust CAS gains are consequently obtained. We confirm that the peak gains which caused the problematic oscillations are reduced in the frequency domain design and the oscillatory motions are indeed suppressed in linear simulations in exchange for slightly slow responses. We finally examine the control performance of our CAS gains in transition phases between different wing tilt angles through human-in-the-loop nonlinear flight simulations with/without wind gust. In both simulations, the roll angle faithfully follows its command in all tilt angles without severe oscillations.

As an extension of our proposed method, we consider the situation in which the probabilistic density of the perturbed models which are used to obtain robust CAS gains is smaller than that of the nominal model. We show that the nominal performance can be improved in exchange for slight performance degradation for perturbed models with small probabilistic density.

Nomenclature

ϕ, θ, ψ: Attitude angles (roll, pitch, and yaw angles, respectively)
τ_w: Wing tilt angle
$G_{\text{lat}}(\tau_w)$: Lateral-directional motion model
$K_{\text{lat}}(\tau_w)$: Primary Flight Control System (PFCS)
k: Controller gain vector
p, r: Attitude rates (roll rate and yaw rate)
T_a, T_{th}: Actuator and motor model time constants
v: Lateral air speed
δ_{flailc}: Flap aileron command
δ_{flrudc}: Flap rudder command
δ_{fllat}: Flaperon angles for lateral-directional motion control
δ_{pwailc}: Power aileron command
δ_{pwrudc}: Power rudder command
δ_{thlat}: Thrust for lateral-directional motion control
δ_{rudc}: Rudder command
$\delta_{\phi\text{stick}}$: Roll stick input
$\delta_{\psi\text{stick}}$: Yaw stick input
$k_{\text{flail}}(\tau_w)$: Flap aileron gain in the Stability Augmentation System (SAS)
$k_{\text{pwail}}(\tau_w)$: Power aileron gain in SAS
$k_{\text{flrud}}(\tau_w)$: Flap rudder gain in SAS
$k_{\text{rud}}(\tau_w)$: Rudder gain in SAS
$k_{\text{pwrud}}(\tau_w)$: Power rudder gain in SAS
$k_{\text{tc}}(\tau_w)$: Turn coordinator gain
$T_{\text{tc}}(\tau_w)$: Turn coordinator time constant
$W(s)$: Weighting function for sensitivity function
$S(s)$: Sensitivity function from attitude command to attitude error
K_{lat}: Admissible CAS gain set for lateral-directional motion control
$k_{\text{p}}(\tau_w)$: Proportional gain in CAS
$k_{\text{i}}(\tau_w)$: Integral gain in CAS
ω_c: Gain crossover frequency
ω_{coff}: Cutoff frequency
c_N: Weighting coefficient for nominal model
c_{Pi}: Weighting coefficient for the ith perturbed model
Clean: Configuration in airplane mode with retracted flaperons.

Data Availability

The data used to support the findings of this study are available from the corresponding author upon request.

Conflicts of Interest

The authors declare that there is no conflict of interest regarding the publication of this paper.

References

[1] T. H. Cox, C. J. Nagy, M. A. Skoog, and I. A. Somers, *Civil UAV Capability Assessment*, NASA TR, 2004.

[2] M. Hassanalian and A. Abdelkefi, "Classifications, applications, and design challenges of drones: a review," *Progress in Aerospace Sciences*, vol. 91, pp. 99–131, 2017.

[3] "Unmanned aircraft systems roadmap: 2005–2030," U.S. Dept. of defense, Office of the Secretary of Defense, 2005, September 2018 https://www.fas.org/irp/program/collect/uav_roadmap2005.pdf.

[4] K. Muraoka, N. Okada, D. Kubo, and M. Sato, "Transition flight of quad tilt wing VTOL UAV," in *28th International Congress of the Aeronautical Sciences, ICAS 2012-11. 1.3*, Brisbane, Australia, 2012.

[5] M. Sato and K. Muraoka, "Flight controller design and demonstration of quad-tilt-wing unmanned aerial vehicle," *Journal of Guidance, Control, and Dynamics*, vol. 38, no. 6, pp. 1071–1082, 2015.

[6] M. Sato and K. Muraoka, "Flight controller design for small quad tilt wing UAV," *Journal of the Japan Society for Aeronautical and Space Sciences*, vol. 64, no. 1, pp. 79–82, 2016.

[7] J. Ackermann, "Multi-model approaches to robust control system design," in *Uncertainty and Control*, J. Ackermann, Ed., vol. 70 of Lecture Notes in Control and Information Sciences, pp. 108–130, Springer, Berlin/Heidelberg, 1985.

[8] J. Kennedy and R. C. Eberhart, *Particle Swarm Optimization, Neural Networks, 1995*, Proceedings., IEEE International Conference on, Perth, WA, Australia, 1995.

[9] Y. Zhang, S. Wang, and G. Ji, "A comprehensive survey on particle swarm optimization algorithm and its applications,"

Mathematical Problems in Engineering, vol. 2015, Article ID 931256, 38 pages, 2015.

[10] M. Jakubcová, P. Máca, and P. Pech, "A comparison of selected modifications of the particle swarm optimization algorithm," *Journal of Applied Mathematics*, vol. 2014, Article ID 293087, 10 pages, 2014.

[11] S. Yavari, M. J. V. Zoej, M. Mokhtarzade, and A. Mohammadzadeh, "Comparison of particle swarm optimization and genetic algorithm in rational function model optimization," *ISPRS - International Archives of the Photogrammetry, Remote Sensing and Spatial Information Sciences*, vol. XXXIX-B1, pp. 281–284, 2012.

[12] C. Nami, K. Oka, A. Harada, and M. Sato, "H_∞ Control-based CAS design of QTW-UAVs using particle swarm optimization," *Transactions of the Japan Society for Aeronautical and Space Sciences*, vol. 61, no. 5, pp. 226–229, 2018.

[13] J. Hu and H. Gu, "Survey on flight control technology for large-scale helicopter," *International Journal of Aerospace Engineering*, vol. 2017, Article ID 5309403, 14 pages, 2017.

[14] F. Mendez-Vergara, I. Cervantes, and A. Mendoza-Torres, "Stability of gain scheduling control for aircraft with highly nonlinear behavior," *Mathematical Problems in Engineering*, vol. 2014, Article ID 906367, 12 pages, 2014.

[15] S. Skogestad and I. Postlethwaite, *Multivariable Feedback Control Analysis and Design Second Edition*, John Wiley& Sons Press, New York, 2001.

[16] I. Maruta, T. H. Kim, and T. Sugie, "Fixed-structure H_∞ controller synthesis: a meta-heuristic approach using simple constrained particle swarm optimization," *Automatica*, vol. 45, no. 2, pp. 553–559, 2009.

[17] A. Banks, J. Vincent, and C. Anyakoha, "A review of particle swarm optimization. Part I: background and development," *Natural Computing*, vol. 6, no. 4, pp. 467–484, 2007.

[18] K. Sedlaczek and P. Eberhard, "Using augmented Lagrangian particle swarm optimization for constrained problems in engineering>using augmented Lagrangian particle swarm optimization for constrained problems in engineering," *Structural and Multidisciplinary Optimization*, vol. 32, no. 4, pp. 277–286, 2006.

[19] K. Latha, V. Rajinikanth, and P. M. Surekha, "PSO-based PID controller design for a class of stable and unstable systems," *ISRN Artificial Intelligence*, vol. 2013, Article ID 543607, 11 pages, 2013.

[20] A. Alfi and H. Modares, "System identification and control using adaptive particle swarm optimization," *Applied Mathematical Modelling*, vol. 35, no. 3, pp. 1210–1221, 2011.